A Furosemide-Sensitive K^+–Cl^- Cotransporter Counteracts Intracellular Cl^- Accumulation and Depletion in Cultured Rat Midbrain Neurons

Wolfgang Jarolimek, Andrea Lewen, and Ulrich Misgeld

I. Physiologisches Institut der Universität Heidelberg, D-69120 Heidelberg, Germany

Efficacy of postsynaptic inhibition through $GABA_A$ receptors in the mammalian brain depends on the maintenance of a Cl^- gradient for hyperpolarizing Cl^- currents. We have taken advantage of the reduced complexity under which Cl^- regulation can be investigated in cultured neurons as opposed to neurons in other *in vitro* preparations of the mammalian brain. Tight-seal whole-cell recording of spontaneous $GABA_A$ receptor-mediated postsynaptic currents suggested that an outward Cl^- transport reduced dendritic $[Cl^-]_i$ if the somata of cells were loaded with Cl^- via the patch pipette. We determined dendritic and somatic reversal potentials of Cl^- currents induced by focally applied GABA to calculate $[Cl^-]_i$ during variation of $[K^+]_o$ and $[Cl^-]$ in the patch pipette. $[Cl^-]_i$ and $[K^+]_o$ were tightly coupled by a furosemide-sensitive K^+–Cl^- cotransport. Thermodynamic considerations excluded the significant contribution of a Na^+–K^+–Cl^- cotransporter to the net Cl^- transport. We conclude that under conditions of normal $[K^+]_o$ the K^+–Cl^- cotransporter helps to maintain $[Cl^-]_i$ at low levels, whereas under pathological conditions, under which $[K^+]_o$ remains elevated because of neuronal hyperactivity, the cotransporter accumulates Cl^- in neurons, thereby further enhancing neuronal excitability.

Key words: Cl^- homeostasis; K^+–Cl^- cotransporter; furosemide; Cl^- depletion; Cl^- accumulation; Donnan equilibrium; cultured neurons

GABA is the main inhibitory transmitter in the mammalian brain. The dominant effect of $GABA_A$ receptor activation is a hyperpolarization caused by Cl^- flux into the cell (for review, see Sivilotti and Nistri, 1991; Kaila, 1994; Thompson, 1994). However, the direction of the Cl^- flux depends on the Cl^- gradient across the membrane. Indeed, $GABA_A$ receptor-mediated hyperpolarizing and/or depolarizing postsynaptic potentials have been observed (for review, see Kaila, 1994; Thompson, 1994). Some findings suggest variations in intracellular $[Cl^-]$ between different neurons and even a distinct Cl^- distribution in different compartments of a single neuron (Misgeld et al., 1986). Depolarizing $GABA_A$ responses, however, can be caused by bicarbonate efflux in combination with Cl^- influx or combined Cl^- and HCO_3^- efflux (Grover et al., 1993; Kaila, 1994; Thompson, 1994; Staley et al., 1995; Perkins and Wong, 1996; Kaila et al., 1997). To be able to predict the direction of Cl^- currents flowing during $GABA_A$ receptor-mediated inhibition it is essential to understand the regulation of Cl^- homeostasis that provides the transmembrane gradient.

A recently cloned K^+–Cl^- cotransporter gene (KCC2) represents a perfect candidate for the regulation of neuronal Cl^- homeostasis (Payne et al., 1996). In contrast to the ubiquitous presence of the K^+–Cl^- cotransporter KCC1, expression of the K^+–Cl^- cotransporter KCC2 is detected in CNS only and seems to be neuron specific. KCC2 is also distinct from KCC1 in that KCC2 is not involved in cell volume regulation and not activated by osmotic changes. Furthermore, KCC2 has a high affinity for extracellular K^+ ions. The properties of KCC2 allow the regulation of $[Cl^-]_i$ to maintain Cl^- gradients for hyperpolarizing GABAergic inhibition. Thermodynamic considerations predict that the electroneutral K^+–Cl^- cotransporter KCC2 operates near equilibrium under physiological ionic conditions. Depending on $[Cl^-]_i$ and $[K^+]_o$ (Payne, 1997), the transport will extrude or accumulate Cl^-.

The functional role of a particular Cl^- transport system in neuronal Cl^- regulation is difficult to establish in studies using integral preparations such as brain slices. One complicating factor is the presence of HCO_3^- anions. The HCO_3^- permeability of the $GABA_A$ channel (Bormann, 1988; Fatima-Shad and Barry, 1993) impedes conclusions toward actual $[Cl^-]_i$ if they are calculated from reversal potentials of $GABA_A$ receptor-mediated anion currents. Furthermore, a HCO_3^-/Cl^- exchanger (Raley-Susman et al., 1993) may well interfere (Chesler, 1990), and pH changes that result from manipulations of $[HCO_3^-]_o$ strongly affect neuronal excitability (Jarolimek et al., 1989; Chesler and Kaila, 1992).

To investigate the functional role of Cl^- transporters we used neuronal cultures that allow measurements of Cl^- reversal potentials under nominally HCO_3^--free conditions. We used patch pipettes to manipulate $[Cl^-]_i$ and tested $[Cl^-]_i$ regulation in somatic and dendritic compartments by varying $[K^+]_o$. The K^+–Cl^- cotransporter KCC2 is furosemide sensitive (Payne, 1997), so we used furosemide to test the inward or outward direction of the Cl^- transport in cultured neurons. We found that a transport with properties of the neuronal-specific K^+–Cl^- cotransporter KCC2 can fully account for Cl^- regulation in cultured midbrain neurons.

Table 1. Composition of extracellular and pipette solutions (in mM)

	Extracellular solutions				Pipette solutions	
	2 K⁺	5 K⁺	8 K⁺	10 K⁺	4.5 mM [A⁻]	15 mM [A⁻]
NaCl	156	153	150	148		3.5
CsCl	1 (5)[a]	1	1	5		
KCl	2	5	8	10		5
K-glucuronate					140	130
CaCl₂	2	2	2	2	0.25	0.25
MgCl₂	1	1	1	1		0.5
Mg-ATP					2	2
Glucose	15	15	15	15	10	10
HEPES	10	10	10	10	10	10
EGTA					5	5
QX 314-Br⁻					4	5

[a]CsCl (5 mM) and K⁺ (10 mM) were used only to record I_{GABA} but not to record sIPSCs to avoid too strong depolarization of network neurons.

MATERIALS AND METHODS

Cell culture. Pregnant Wistar rats were anesthetized by ether inhalation and killed by decapitation. The embryos were removed, placed in sterile, ice-cold Gey's buffered salt solution containing (in mM): NaCl 137, KCl 5, MgSO₄ 0.3, NaH₂PO₄ 1, CaCl₂ 1.5, NaHCO₃ 2.7, KH₂PO₄ 0.2, MgCl₂ 1, glucose 5, at pH 7.4, and immediately decapitated. Pieces of ventral midbrain tissue from the 14-d-old embryos were mechanically dissociated and plated on a primary culture of glial cells from the same area. Cell culture conditions were as described previously (Bijak et al., 1991; Jarolimek and Misgeld, 1992). Cells used in this study were 4–8 weeks in

culture. Immunocytochemistry studies have shown that this culture preparation contains ~5% dopaminergic neurons and <5% serotonergic neurons (Rohrbacher et al., 1995) in addition to ~70% GABAergic neurons (our unpublished results). The fact that EPSPs attributable to activation of glutamatergic receptors comprise a significant proportion of the observed postsynaptic activity (Bijak et al., 1991) suggests that most non-GABAergic neurons possess a glutamatergic neurotransmitter phenotype.

Electrophysiological recordings. Recordings were performed at room temperature (22–25°C) in the whole-cell voltage-clamp configuration

Figure 1. GABAergic network neurons generated inward and outward IPSCs in a single target neuron through GABA_A receptors. *A1*, Spontaneous IPSCs were inward and outward current transients in a cell recorded at V_H −63 mV. Inward and outward sIPSCs occurred in isolation (*1*), or inward currents were curtailed by outward sIPSCs (*2*). Note the difference in calibration between 1 and 2. *A3*, In another cell inward sIPSCs occurred in clusters interrupted by "silent" periods, whereas outward sIPSCs occurred rather continuously (V_H −71 mV). *B*, The GABA_A antagonist bicuculline (*bic*) reversibly blocked all inward and outward sIPSCs. *a, b,* Expanded segments of the top trace where indicated. *C, D,* Inward and outward sIPSCs differed in their time courses. Inward (*D1*) and outward (*C1*) sIPSCs that occurred in separation could be fitted by a single exponential function (*solid line*; V_H −63 mV). For the sIPSCs shown, the time constant of decay was 26.2 msec (amplitude coefficient 39.4) and 6.0 msec (amplitude coefficient −33.1). For analysis, only sIPSCs that had no inflections in the rise or decay phase were accepted. Rise time (10–90%) histogram of all inward (*D2*) and outward (*C2*) sIPSCs showed that rise time was slower for outward sIPSCs. Similarly, histograms of decay time constant (*C3, D3*) revealed a much slower decay for outward sIPSCs (*C3*). For the histograms, 31 outward and 45 inward IPSCs (sampled in 1 min) were analyzed. All recordings in this Figure were obtained in the presence of ionotropic glutamate receptor antagonists and of 2 mM [K⁺]_o ([A⁻]_pip 15 mM).
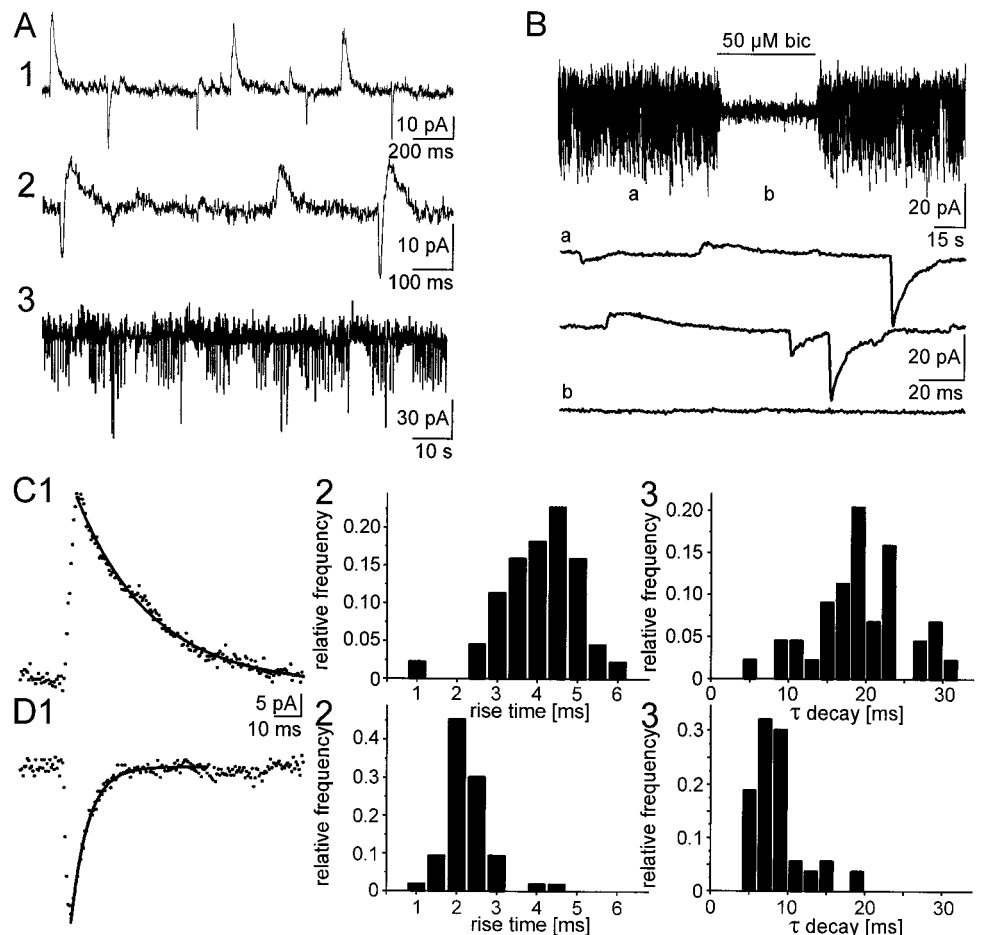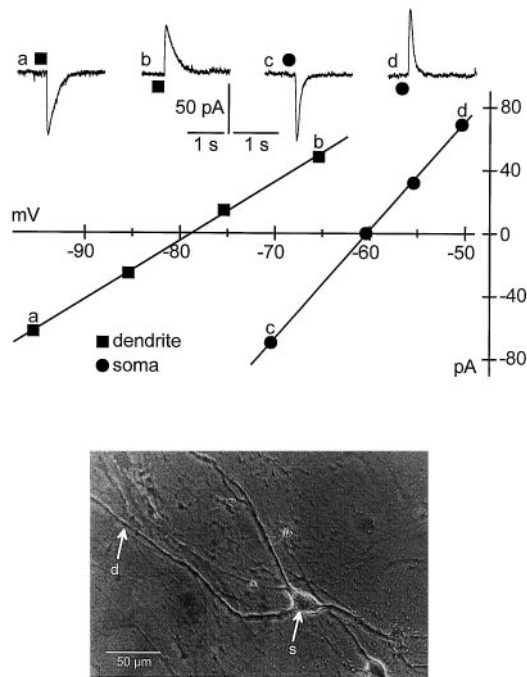
Figure 2. Dendritic and somatic GABA applications generated Cl^- currents with different reversal potentials. In the same cell, currents induced by focal application of GABA (1 mM) to a dendrite (■) or the soma (●) had different reversal potentials. Application sites as shown for a cell in the *inset* (*s*, somatic; *d*, dendritic). Recording conditions were 2 mM $[K^+]_o$ and 15 mM $[A^-]_{pip}$. *Letters* mark the points on the current–voltage relationship at which the sample currents shown above had been recorded. *Symbols* represent the mean of three consecutive applications. Note the voltage range at which GABA evoked an outward current in the dendrite and an inward current at the soma.

with a patch-clamp amplifier (L/M-EPC 7, List, Darmstadt, Germany). The composition of the extracellular solutions and the patch pipette solutions are given in Table 1. No CO_2 or O_2 was added, and the pH of all solutions was adjusted to 7.3. Glucuronate salts were used because the permeability of the anion through $GABA_A$ channels should be small because of its restricted, bulky conformation. 5-*N*-(2,6-dimethyl-phenylcarbamoylmethyl)-triethylammonium bromide (QX314) was added to the intracellular solution to block Na^+ and K^+ currents (Connors and Prince, 1982; Nathan et al., 1990; Colling and Wheal, 1994). The Br^- salt was used because in initial experiments the block of action potentials was faster and more complete with Br^- than with the Cl^- salt. Br^- has a permeability similar to that of Cl^- at $GABA_A$ channels (Bormann, 1988); therefore, concentrations of permeable ions used for calculations were the sum of Cl^- and Br^- concentrations. The reliability of this approach was tested by replacement of 5 mM $[Cl^-]_o$ by 5 mM $[Br^-]_o$ to obtain an identical $[Br^-]$ in the extracellular solution and the patch pipette. This change had no measurable influence on reversal potentials of GABA-induced currents ($n = 4$). We did not replace K^+ by Cs^+ in the patch pipette because Cs^+ could interfere with the presumed K^+–Cl^- cotransporter competing with K^+ for the internal binding site and/or changing the driving force for the transporter. CsCl was added, however, to the extracellular solution to reduce leak conductance. In preliminary experiments we tested whether extracellular Cs^+ affected the K^+–Cl^- cotransporter. Furosemide (0.1 mM) shifted the dendritic reversal potential (E_{GABA}) of GABA-induced currents (I_{GABA}) in a positive direction at 2 mM $[K^+]_o$ and in a negative direction at 10 mM $[K^+]_o$ and low $[Cl^-]_{pip}$ (see Results). Neither dendritic E_{GABA} nor its shifts that were induced by furosemide changed when we added 5 mM Cs^+ ($n = 5$), suggesting that Cs^+ was not a substrate for the transporter and did not compete for the extracellular binding site of K^+. Therefore the extracellular solution always contained 5 mM Cs^+ to reduce leak conductance when we measured reversal potentials for GABA currents. Spontaneous synaptic activity in the embryonic midbrain culture consists of EPSCs that are blocked by the AMPA-type glutamate antagonist

6,7-dinitroquinoxaline-2,3-dione (DNQX) and IPSCs sensitive to antagonists for the $GABA_A$ receptors bicuculline or picrotoxin (Bijak et al., 1991; Jarolimek and Misgeld, 1991). To block excitation, DNQX (20 μM) and the NMDA receptor-type antagonist DL-2-amino-4-methyl-5-phosphono-3-pentenoic acid (1 μM) were present in all extracellular recording solutions.

Patch pipettes were fabricated from borosilicate glass (Hilgenberg, Malsfeld, Germany), and their resistances to bath ranged from 2 to 4 MΩ. The access resistance was estimated from the amplitude of the capacitive current evoked by a hyperpolarizing 10 mV step. Access resistances varied between 5 and 12 MΩ and were routinely checked during the recording. No series resistance or slow capacitance compensation was used during the experiment because currents were measured >15 sec after the membrane potential was changed. Given the small amplitude (<200 pA) of the recorded currents, series resistance error was <2.5 mV. The liquid junction potential between the patch pipette and the extracellular solution was calculated according to Barry and Lynch (1991). The calculation yielded 15.8 and 17.5 mV for 15 and 4.5 mM $[A^-]_{pip}$, respectively. When measured according to the procedure described by Neher (1992), the values were 14.0 and 15.5 mV, respectively, which are in good agreement with the calculated values. Because it has been suggested that calculated rather than measured values be used (Barry and Lynch, 1991), all potentials reported in this paper have been corrected for the calculated liquid junction potentials.

Recordings were started >5 min after the whole-cell configuration was established to allow adequate time for QX314 to take effect and for anions to equilibrate. After 5 min, no further change in dendritic or somatic E_{GABA} was observed. GABA (1 mM) was applied by pressure ejection (1–20 kPa, 20–40 msec) every 15 sec from a pipette with a <1 μm opening. I_{GABA} was measured in the presence of tetrodotoxin (0.3 μM) to avoid superposition of I_{GABA} and action potential-dependent IPSCs as well as the activation of fast Na^+ currents in the recorded cell. All inorganic salts were of analytical grade (Merck, Darmstadt, Germany). Drugs were from Sigma (Deisenhofen, Germany) except DNQX and tetrodotoxin (RBI, Köln, Germany).

Extracellular solutions were applied by a multibarrel perfusion system that was positioned ~250 μm away from the soma of the recorded cell (Bijak et al., 1991; Jarolimek and Misgeld, 1992).

Data analysis. Recordings were filtered at 1.3–3 kHz with a four-pole Bessel filter, acquired and analyzed with pClamp (Axon Instruments, Foster City, CA) hardware and software, and additionally stored on a DAT recorder. The time course and amplitude of spontaneous IPSCs (sIPSCs) were analyzed with a program written in our laboratory (Jarolimek and Misgeld, 1997; Rohrbacher et al., 1997). The reversal potential of I_{GABA} was determined by linear regression of the current–voltage relationship. Currents were recorded at holding potentials (V_H) on both sides of E_{GABA}. After 15–45 sec at a new V_H, the current amplitudes induced by three consecutive applications were averaged. Despite the rapid exchange of the extracellular solution (~0.5 sec) around the neuron, effects were determined >1 min after the start of the application to achieve steady-state conditions. Theoretical $[Cl^-]_i$ of the neuron was calculated with the Nernst equation using measured E_{GABA} values and $[Cl^-]_o$ values given in Table 1. Calculated values were not corrected for the presence of Br^- in the pipette and in the neuron. The driving force for the K^+–Cl^- cotransporter was estimated on the basis of the Nernst equation given the calculated $[Cl^-]_i$ and $[K^+]_o$ from Table 1. Data are reported as mean ± SEM.

RESULTS

Cl⁻ gradient between soma and dendrites

When tight-seal whole-cell recordings were performed under conditions of 15 mM permeant anions in the patch pipette ($[A^-]_{pip}$), 2 mM $[K^+]_o$, and pharmacological blockade of ionotropic glutamate receptors, sIPSCs did not reverse in sign at a defined holding potential (V_H). Instead, at V_H in a range near the reversal potential ($E_{Cl} = -61$ mV as determined from the Nernst equation), inward and outward sIPSCs concurred in 46 of 51 cells (Fig. 1*A*). All sIPSCs were blocked by bicuculline ($n = 5$), suggesting that they were mediated by $GABA_A$ receptors (Fig. 1*B*). Inward and outward sIPSCs appeared to be separated (Fig. 1*A1*) or as sequences of inward currents curtailed by outward currents (Fig. 1*A2*). As shown in Figure 1*A3*, another pattern

Table 2. Summary of E_{GABA} measured under various $[K^+]_o$ and $[A^-]_{pip}$

	Dendrite		Soma	
	Control	Furosemide (0.1 mM)	Control	Furosemide (0.1 mM)
$[A^-]_{pip}$ (15 mM)	2 mM $[K^+]_o$			
	-75.7 ± 1.8 (20)	-65.0 ± 1.5 (12)	-59.8 ± 1.1 (16)	-57.5 ± 1.1 (9)
	10 mM $[K^+]_o$			
	-63.0 ± 0.9 (6)	-59.9 ± 0.6 (6)	-56.5 ± 0.3 (4)	-56.3 ± 0.3 (3)
$[A^-]_{pip}$ (4.5 mM)	2 mM $[K^+]_o$			
	-97.7 ± 1.8 (9)	-90.3 ± 2.5 (6)	-83.4 ± 0.9 (13)	-79.2 ± 1.0 (9)
	10 mM $[K^+]_o$			
	-72.5 ± 2.1 (9)	-76.8 ± 1.4 (8)	-73.7 ± 0.9 (6)	-76.7 ± 1.0 (7)

GABA (1 mM) was pressure-applied from a patch pipette with a tip diameter of <1 μm. Dendritic applications were >150 μm apart from soma. Reversal potentials were determined from current–voltage plots in which each point was the average of three applications, and the linear regression was calculated from three to seven data points on both sides of E_{GABA}. Mean values $\pm$ SEM are given for the number of cells indicated in brackets. Values are corrected for liquid junction potentials.

consisted of clustered inward sIPSCs that were accompanied by a continuous barrage of outward sIPSCs or vice versa. We analyzed the time courses of apparently isolated inward and outward sIPSCs in a single cell at a V_H at which amplitudes of inward and outward IPSCs were in a similar range (Fig. 1*C,D*). There was a clear difference in the time courses. Outward sIPSCs consistently had a slower rise time and time constant of decay than inward sIPSCs (rise time, 1.9 ± 0.1 msec vs 5.3 ± 0.4 msec; decay time constant, 16.2 ± 1.3 msec vs 38.6 ± 4.8 msec for inward and outward sIPSCs, respectively; $n = 5$ cells). On the basis of these observations, we assumed that outward sIPSCs were generated in dendritic compartments but that inward sIPSCs were generated near soma. Presynaptic GABAergic neurons of the network would generate inward and outward IPSCs if they formed synapses with all parts of the somatodendritic surface. Presynaptic neurons contacting restricted areas either near soma or in apical dendrites would generate a continuous barrage or clusters of inward or outward IPSCs consistent with their firing mode,

continuous or in bursts. Assuming further that under the given recording conditions in the culture (see Discussion) soma and dendrites did not deviate considerably from isopotentiality, we had to postulate $[Cl^-]_i$ to be lower in dendritic than in somatic compartments.

To examine compartmental differences in $[Cl^-]_i$ we applied GABA (1 mM) focally to somatic and dendritic regions (Fig. 2). To provide comparable conditions of origin for sIPSCs and GABA-evoked currents (I_{GABA}), application was adjusted so that the amplitude of I_{GABA} was in the range of amplitudes of sIPSCs. When tested in a voltage range around the reversal potential ($E_{GABA} \pm 25$ mV), slope conductances of dendritic and somatic I_{GABA} were linear (Fig. 2). However, slope conductance was smaller for dendritic than for somatic applications, and often pressure or application time for the focal application had to be increased to obtain a measurable dendritic I_{GABA}. The difference was probably caused by different density of receptors and/or surface size facing the application pipette if GABA was applied
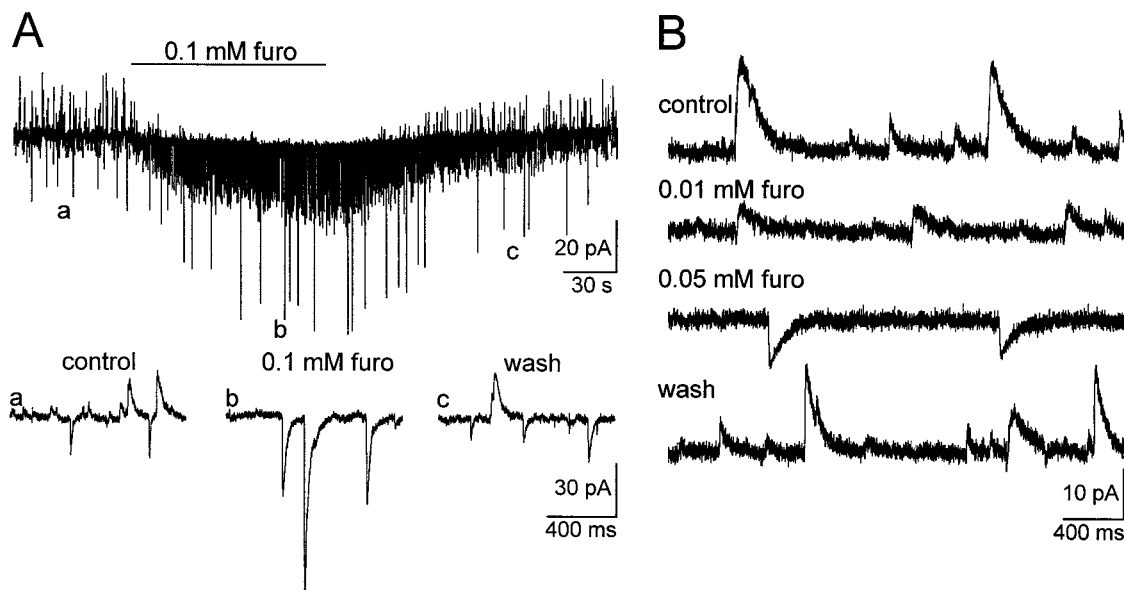
Figure 3. Furosemide changed the reversal potential of sIPSCs. *A*, Spontaneous IPSCs were inward and outward at V_H of -61 mV. Furosemide (*furo*; 0.1 mM) increased the frequency and amplitude of inward sIPSCs (recorded in 2 mM $[K^+]_o$, 15 mM $[A^-]_{pip}$), whereas outward sIPSCs disappeared. The onset of the furosemide effect is already seen after 10 sec, and the effect is reversible. *Letters* mark time points that are shown at higher sweep speed in the lower traces. *B*, In another cell under otherwise identical recording conditions as in *A*, V_H was set to record outward sIPSCs. Application of increasing concentrations of furosemide first reduced the amplitude of outward sIPSCs and then reversed sign of sIPSCs.
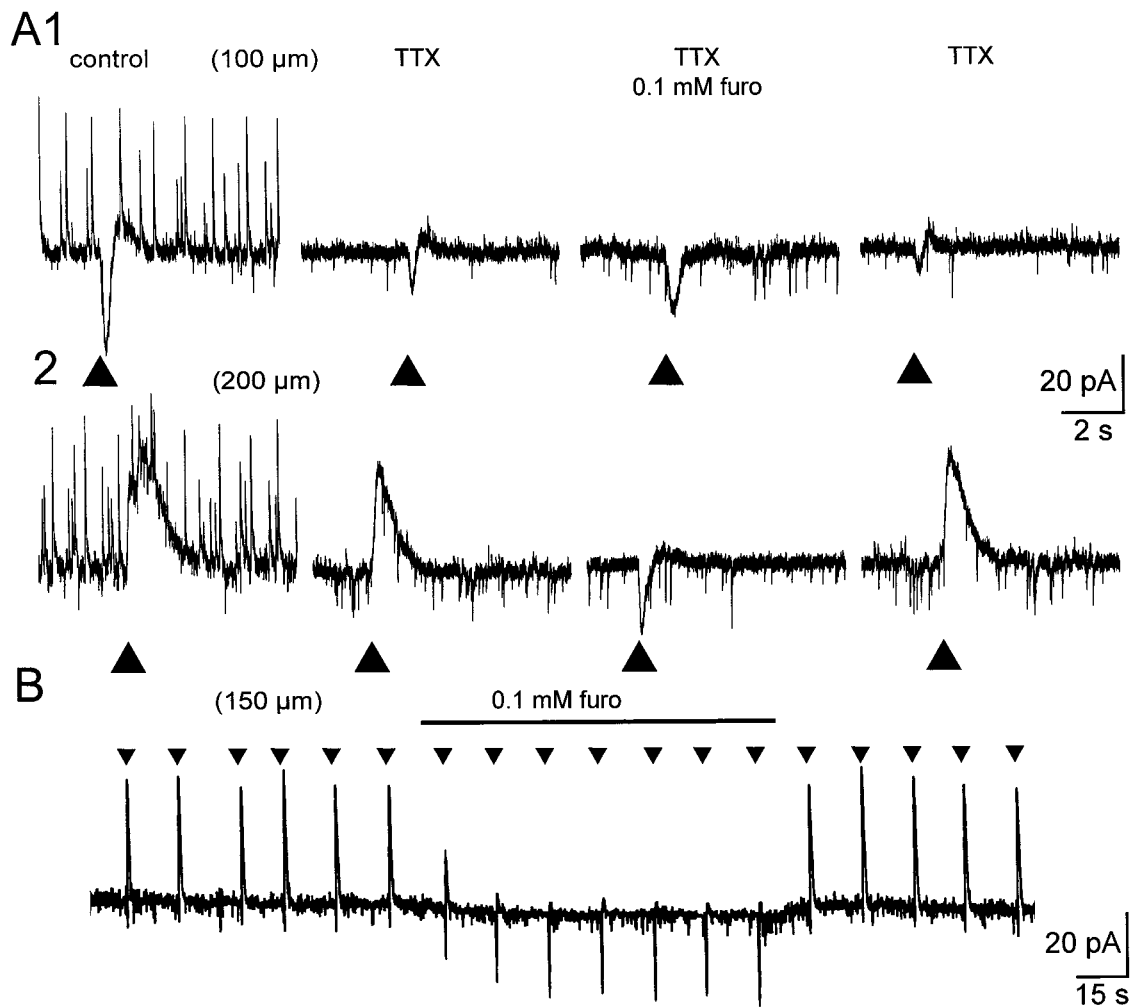
Figure 4. Furosemide affected the reversal potential of dendritic I_{GABA} more strongly than of somatic I_{GABA}. *A*, Pressure ejection of GABA (▲) (distance to the soma is given in *parentheses*) induced an inward current when applied close to the soma (*A1*) but an outward current in dendrites (*A2*). Under control recording conditions (15 mM $[A^-]_{pip}$; 2 mM $[K^+]_o$; V_H −66 mV), sIPSCs were recorded at a V_H at which outward sIPSCs predominated. In the presence of tetrodotoxin (*TTX*) to eliminate sIPSCs, furosemide reversed the current direction of dendritic I_{GABA} (*A2*), whereas the amplitude of somatic I_{GABA} was increased only slightly (*A1*). Both effects were completely reversible. To obtain a clear signal in presence of sIPSCs, slightly larger ejection pressure was used than was needed in TTX. *B*, Chart recording of the time course of the furosemide-induced shift of E_{GABA}. In the same cell as in *A*, dendritic I_{GABA} measured in TTX reversed current direction on application of furosemide. This effect readily reversed on washout.

near soma or near dendrites. As expected from the observation of inward and outward sIPSCs, dendritic I_{GABA} (application >100 μm away from soma) was outward at a V_H at which somatic I_{GABA} of the same cell was inward (Fig. 2). In a singe cell, E_{GABA} differed by up to 25 mV (mean 12.9 ± 2.3 mV; $n = 9$) between soma and dendrites (Table 2).

Dependence of the somatodendritic Cl⁻ gradient on a furosemide-sensitive transport

Calculation of inorganic $[A^-]_i$ from E_{GABA} values reported above revealed that dendritic $[A^-]_i$ was lower than somatic $[A^-]_i$. If dendritic $[Cl^-]_i$ was lowered by a furosemide-sensitive transport, it should be possible to reduce the somatodendritic $[Cl^-]$ gradient by furosemide application. Therefore, we tested the effects of furosemide on sIPSCs and I_{GABA}. Furosemide altered the driving force for sIPSCs. At V_H near the expected E_{IPSC}, amplitudes of inward sIPSCs increased and those of outward sIPSCs decreased or they reversed in sign (Fig. 3*A*). A new apparent steady state was achieved after maximally 1 min, and the effect of furosemide was fully reversible in a similar time. Effects

of furosemide were observed at concentrations as low as 10 μM (Fig. 3*B*; $n = 4$ of 5 cells) and increased in a concentration-dependent manner ($n = 9$). The maximal concentration we used in all further experiments was 0.1 mM to avoid unspecific effects of furosemide (Cabantchik and Greger, 1992). To quantify the effect of furosemide on E_{GABA}, current–voltage relationships for I_{GABA} were determined in the presence and absence of furosemide (0.1 mM). In one series of experiments ($n = 15$), the position of the application pipette was guided by the current direction of sIPSCs. First, the range of V_H was determined at which inward and outward sIPSCs were measurable. Thereafter, a V_H at the positive side of this range was chosen to record predominantly outward sIPSCs that were likely generated in dendritic compartments (Fig. 4*A1*). In this situation the position of the application pipette was chosen so that I_{GABA} was inward. In most instances the compartment reached from the soma up to 100 μm away from the somatic patch pipette for smoothly tapering dendrites (Fig. 2, *inset*). At a distance from soma of ~200 μm, current direction of I_{GABA} and sIPSCs concurred (Fig. 4*A2*).
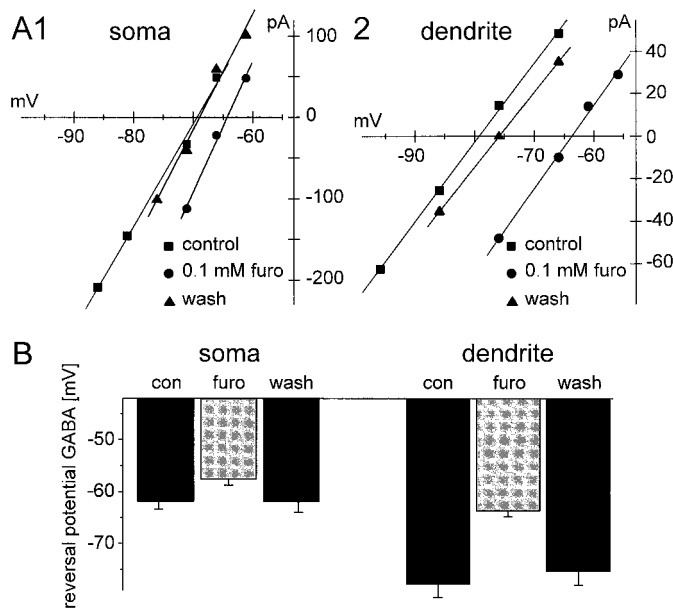
Figure 5. Furosemide reduced the difference of reversal potentials of I_{GABA} between dendrites and soma. *A*, Current–voltage relationship of somatic (*A1*) and dendritic (*A2*) I_{GABA} could be fitted by a linear regression line (15 mM $[A^-]_{pip}$ and 2 mM $[K^+]_o$). Furosemide shifted the current–voltage relationship to more positive values, whereas the slope conductance was unchanged. The effect was reversible on washout. E_{GABA} in the absence of furosemide was more negative for dendritic I_{GABA} than for somatic I_{GABA}. In furosemide, the difference between dendritic and somatic E_{GABA} was small, indicating that the change of E_{GABA} was more pronounced at the dendrites than at the soma. *B, Bar charts* summarize mean E_{GABA} (and SEM) for the different recording conditions. The number of cells is nine for somatic I_{GABA} and six for dendritic I_{GABA}.

Furosemide only slightly increased the amplitude of somatic I_{GABA} (Fig. 4*A1*), whereas dendritic I_{GABA} reversed in sign (Fig. 4*A2*). As shown in Figure 4*B*, a new steady-state for dendritic I_{GABA} was achieved within 30–45 sec. The effect of furosemide was fully reversible. The data indicate a pronounced shift of E_{GABA} under furosemide in dendrites but not at the soma.

In another set of experiments, furosemide (0.1 mM)-induced shifts in E_{GABA} were quantified for dendritic (application ~200 μm apart from soma) and somatic I_{GABA}. As shown in Figure 5*A*, furosemide shifted dendritic and somatic E_{GABA} in positive direction but did not reduce slope conductance. This suggests that furosemide changed $[A^-]_i$ but had no blocking action on GABA$_A$ receptors. Furosemide (0.1 mM) shifted somatic E_{GABA} less than dendritic E_{GABA} (4.2 ± 1.0 mV vs 11.8 ± 1.4 mV; $n = 8$) (Fig. 5*B*), with the result that furosemide reduced the somatodendritic inorganic $[A^-]$ gradient. These findings showed that at 15 mM $[A^-]_{pip}$ and 2 mM $[K^+]_o$ the somatic inorganic $[A^-]_i$ was mainly governed by A^- diffusion from the patch pipette into the cytoplasm of the cell body. Dendritic inorganic $[A^-]$ was significantly lowered with respect to somatic $[A^-]_i$ by the operation of a furosemide-sensitive Cl⁻ outward transport.

Dependence of the direction of the Cl⁻ transport on $[K^+]_o$ and $[Cl^-]_i$

The concentrations of furosemide used in our study inhibit the K⁺–Cl⁻ cotransporter (KCC2) in heterologous expression systems. At concentrations of $[Cl^-]_i$ (4–10 mM) and $[K^+]_o$ (2–10 mM) that can be expected to occur in the mammalian brain, KCC2 operates near its thermodynamic equilibrium. The direction of

Cl⁻ transport depends on $[Cl^-]_i$ and $[K^+]_o$ (Payne, 1997). We tested whether these characteristics also apply to the regulation of Cl⁻ homeostasis in neurons.

I_{GABA} at 15 mM $[A^-]_{pip}$

Increasing $[K^+]_o$ from 2 to 10 mM shifted dendritic E_{GABA} to positive values (Table 2). An apparent, new steady state was attained only after the inward current elicited by $[K^+]_o$ had peaked (Fig. 6*A1*). When measured at 2 and 10 mM $[K^+]_o$ in the same cells, the shift of dendritic E_{GABA} mounted to 16.5 ± 3.3 mV ($n = 3$). In 10 mM $[K^+]_o$, furosemide (0.1 mM) shifted dendritic E_{GABA} to even more positive values (3.3 ± 0.7 mV; $n = 4$), but the shift was consistently smaller than it had been at 2 mM $[K^+]_o$ (11.8 ± 1.4 mV; $n = 8$) (Fig. 6*A2–A4*). This result corresponds to the expected diminution of the driving force for the K⁺–Cl⁻ cotransporter at high $[K^+]_o$. Assuming that somatic inorganic $[A^-]$ was dominated by $[A^-]_{pip}$, elevation of $[K^+]_o$ should not result in large changes in somatic E_{GABA}. As expected, increasing $[K^+]_o$ from 2 to 10 mM hardly changed somatic E_{GABA} (1.0 ± 0.5 mV; $n = 3$) when tested in the same cells, and furosemide had no effect on somatic E_{GABA} at 10 mM $[K^+]_o$ (Table 2). Consequently, in 10 mM $[K^+]_o$ and furosemide, there was little if any somatodendritic gradient for inorganic $[A^-]$.

I_{GABA} at 4.5 mM $[A^-]_{pip}$

In the experiments presented above, the patch pipette was used to load the somatic compartment with moderate inorganic $[A^-]$. To evaluate the role of $[Cl^-]_i$, we lowered $[A^-]_{pip}$ (4.5 mM). With 4.5 mM $[A^-]_{pip}$, dendritic I_{GABA} was more negative than with 15 mM $[A^-]_{pip}$ (Table 2). According to the smaller driving force for the K⁺–Cl⁻ cotransporter at 4.5 mM $[A^-]_{pip}$ and 2 mM $[K^+]_o$, the furosemide (0.1 mM)-induced shift of dendritic E_{GABA} was small (7.0 ± 0.9 mV; $n = 6$) (Fig. 6*B*). Increasing $[K^+]_o$ from 2 to 10 mM strongly shifted dendritic E_{GABA} to positive values (27.8 ± 2.8 mV; $n = 6$). At 10 mM $[K^+]_o$, furosemide induced small shifts of dendritic E_{GABA}; however, they were in the direction opposite to the shifts in 2 mM $[K^+]_o$ (−5.0 ± 0.7 mV; $n = 7$) (Fig. 6*B*). These data indicate that at low $[A^-]_{pip}$ the direction of the Cl⁻ transport in the dendrites had been reversed by elevating $[K^+]_o$. At 2 mM $[K^+]_o$, $[A^-]_{pip}$ and the furosemide-sensitive Cl⁻ *outward* transport determined dendritic $[Cl^-]_i$, whereas at 10 mM $[K^+]_o$, dendritic $[Cl^-]_i$ was governed by the Gibbs–Donnan equilibrium and the furosemide-sensitive *inward* transport.

We next tested the effects of $[K^+]_o$ changes on somatic E_{GABA} at low $[A^-]_{pip}$. At 2 mM $[K^+]_o$, somatic E_{GABA} was more positive than dendritic E_{GABA} (Table 2). However, elevation of $[K^+]_o$ and application of furosemide (0.1 mM) had effects similar to those on dendritic E_{GABA} (Table 2). At 2 mM $[K^+]_o$, furosemide shifted somatic E_{GABA} to more positive values (4.2 ± 0.5 mV; $n = 8$). Elevating $[K^+]_o$ from 2 to 10 mM shifted somatic E_{GABA} in the same direction (7.0 ± 0.1 mV; $n = 4$) and reversed the shift of somatic E_{GABA} under furosemide (−3.4 ± 0.6 mV; $n = 6$). In 10 mM $[K^+]_o$, therefore, no somatodendritic gradient for inorganic $[A^-]_i$ existed in either the presence or absence of furosemide.

sIPSCs

Finally, we tested whether inward and outward sIPSCs were altered by $[Cl^-]_i$, $[K^+]_o$, and furosemide as expected from the data reported on I_{GABA}. At 2 mM $[K^+]_o$ and low $[A^-]_{pip}$, the mean amplitude of sIPSCs measured at different V_H could not be fitted by a linear regression because sIPSCs appeared as inward and outward currents near E_{IPSC} ($n = 4$) (Fig. 7*A*). Increasing $[K^+]_o$ from 2 to 5 mM while recording from the same cell allowed
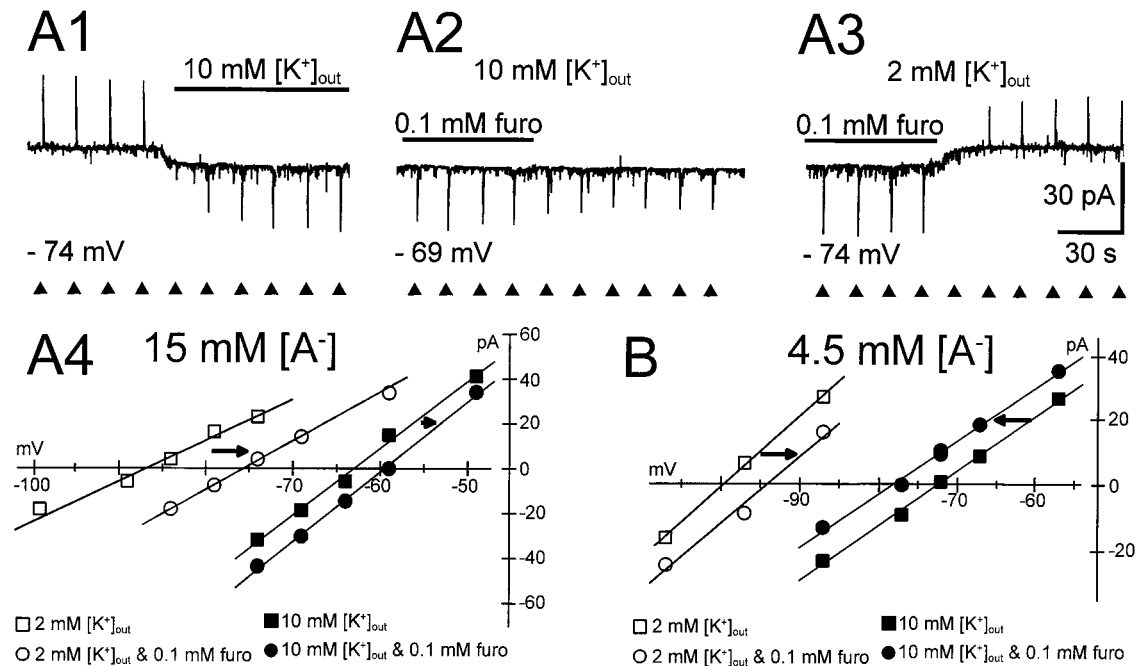
Figure 6. The furosemide-sensitive K^+–Cl^- cotransporter extruded or accumulated Cl^- depending on $[K^+]_o$ and $[Cl^-]_i$. *A*, The shift of dendritic E_{GABA} induced by furosemide was larger in 2 mM $[K^+]_o$ than in 10 mM $[K^+]_o$ when $[A^-]_{pip}$ was high (15 mM). *A1*, Elevating $[K^+]_o$ from 2 to 10 mM shifted E_{GABA} of dendritic I_{GABA} (▲ marks application of GABA) to positive values, which resulted in a reversal of current direction (V_H is indicated below chart records). Washout of furosemide had only a small effect on I_{GABA} in 10 mM $[K^+]_o$ (*A2*) but a strong effect in 2 mM $[K^+]_o$. *A4*, Current–voltage relationship for the cell shown in *A1–A3*. For clarity, control and recovery data were pooled. *Arrows* indicate direction of the shift in dendritic E_{GABA}. *B*, In another cell recorded with low $[A^-]_{pip}$ (4.5 mM), furosemide induced a small positive shift at 2 mM $[K^+]_o$ but a small negative shift of dendritic E_{GABA} at 10 mM $[K^+]_o$.

the current–voltage relation to be fitted by a first order regression because the sIPSCs reversed in sign at a defined V_H (Fig. 7*B*). At 5 mM $[K^+]_o$, the ratio of $[Cl^-]_o/[Cl^-]_i$ approximately equaled $[K^+]_i/[K^+]_o$; hence no driving force for an electroneutral K^+–Cl^- cotransport existed, leading to a collapse of the somatodendritic $[A^-]$ gradient. Furthermore, the time course of inward IPSCs measured near the reversal potential became slower in 5 mM $[K^+]_o$ than apparent inward IPSCs had been in 2 mM $[K^+]_o$ in the same cell (rise time, 1.48 ± 0.04 msec vs 1.00 ± 0.04 msec; time constant of decay, 16.5 ± 0.1 msec vs 7.1 ± 0.3 msec for 59 inward sIPSCs in 5 mM $[K^+]_o$ and 37 inward sIPSCs in 2 mM $[K^+]_o$ at V_H −77 and −87 mV, respectively). As expected from the thermodynamic properties of the K^+–Cl^- cotransporter, increasing $[K^+]_o$ to 8 mM at 4.5 mM $[A^-]_{pip}$ reversed the transport direction of the Cl^- transport. Under these conditions, furosemide decreased the amplitude of inward sIPSCs and increased the amplitude of outward sIPSCs (*n* = 3) (Fig. 8). The changes were the opposite of the changes induced by furosemide at 15 mM $[A^-]_{pip}$ and low $[K^+]_o$ (Fig. 3*A*).

DISCUSSION

Our data show that a furosemide-sensitive transport can accumulate or extrude Cl^- from embryonic midbrain neurons in long-term culture. In terms of sensitivity to furosemide and to changes in $[Cl^-]_i$ and $[K^+]_o$, the cotransporter exhibits functional characteristics described for the neuronal K^+–Cl^- cotransporter isoform (KCC2) expressed in human embryonic kidney cell lines (Payne, 1997). Because of the properties of the electroneutral K^+–Cl^- cotransporter, $[K^+]_o$ determines the driving force for Cl^- fluxes across GABA$_A$ receptor channels and hence regulates synaptic inhibition.

Reduction of a $[Cl^-]_i$ gradient between dendrites and soma by furosemide or $[K^+]_o$

We observed a striking difference in driving forces for GABA$_A$ currents between cell soma and dendrites. Both, bicuculline-sensitive sIPSCs and focal GABA applications revealed the gradient. At a V_H near the expected equilibrium potential for Cl^-, GABA$_A$ currents were inward near soma and outward in dendritic parts. Furosemide reduced the somatodendritic differences in the driving forces, inducing a shift in E_{GABA} that was more pronounced for dendritic currents than for somatic currents. A reduction of the somatodendritic gradient was also observed if $[K^+]_o$ was increased or $[A^-]_{pip}$ was reduced.

Dendritic $[Cl^-]_i$ resulting under our experimental conditions (Fig. 9*A*) can be explained from Gibbs–Donnan equilibrium and the thermodynamic profile of an electroneutral K^+–Cl^- cotransport (Fig. 9*B*). K^+ and Cl^- can be expected to be nearly in equilibrium across the neuronal membrane. $[Cl^-]_i$ equal to $[K^+]_o$ approximately satisfied the Donnan relationship as well as the principle of electroneutrality. $[Cl^-]_i$ was actually increased above $[Cl^-]_i$ predicted from the Donnan relationship or reduced below that concentration by a higher or lower $[Cl^-]_{pip}$, respectively. Near soma, $[Cl^-]_{pip}$ determined $[Cl^-]_i$ more closely than in the dendrites. Depending on $[K^+]_o$, dendritic $[Cl^-]_i$ was lower (Fig. 9*Aa–Ac*) or higher (Fig. 9*Ad*) than somatic $[Cl^-]_i$, indicating that Cl^- movement across conductivity pathways exceeded Cl^- diffusion from the patch pipette. The electroneutral K^+–Cl^- cotransporter contributed to the conductivity pathways according to its energy profile (Fig. 9*B*), as revealed by the shift in dendritic $[Cl^-]_i$ resulting from furosemide application. When $[K^+]_o$ was low and $[Cl^-]_{pip}$ was high (Fig. 9*Aa*), the driving force for the
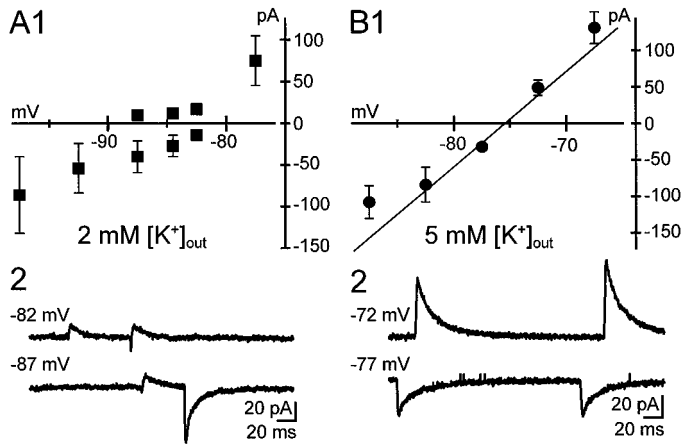
Figure 7. Near the thermodynamic equilibrium of the K^+–Cl^- cotransporter, GABAergic network neurons generated sIPSCs with the same reversal potential at the soma and the dendrites of the target neuron. *A,* In a cell (4.5 mM $[A^-]_{pip}$), inward and outward sIPSCs occurred at a V_H −80 to −90 mV. Current–voltage relationship for the sIPSCs was determined by sampling peaks of inward or outward currents, respectively (*A1*). *A2,* Traces show representative examples for inward and outward sIPSCs at two V_H values that were 5 mV apart. *B1,* In the same cell as in *A,* the current–voltage relationship for peaks of all sIPSCs could be well fitted by a linear regression line ($r = 0.96$) at 5 mM $[K^+]_o$. In the plots, mean values and SE bars are shown unless SE bars remained within symbol sizes. Minimum to maximum of sIPSC numbers sampled at each V_H ranged from 48 to 132.

K^+–Cl^- cotransporter was sufficiently large to generate a pronounced somatodendritic gradient. The somatodendritic gradient was built up by the solution in the patch pipette, which served as a Cl^- source, and the K^+–Cl^- cotransporter, which counteracted that Cl^- load. The development of a Cl^- gradient allowed us to study Cl^- regulation, but the experiments did not determine under which conditions such a gradient may exist in intact neurons.

$[Cl^-]_i$ calculated from somatic E_{GABA} was always somewhat higher than $[Cl^-]_{pip}$. The small deviation was likely attributable to injected currents carried by anions because we set V_H negative to the membrane potential. Supporting this suggestion, the relative increase of $[Cl^-]_i$ above $[Cl^-]_{pip}$ was larger with $[Cl^-]_{pip}$ of 4.5 mM than with $[Cl^-]_{pip}$ of 15 mM. The low mobility of the main anion glucuronate promoted an increase of $[Cl^-]_i$ above $[Cl^-]_{pip}$. Other possible factors such as production of endogenous CO_2 or the use of Br^- were less likely contributors. An equal pH inside

and outside the cells probably prevented buildup of a HCO_3^- gradient, and removal of the gradient for Br^- had no measurable effect on E_{GABA} (see Materials and Methods).

The observed fast and slow sIPSCs could represent an artifact of an imperfect space clamp. A similar finding was reported for $GABA_A$ responses in CA1 neurons of hippocampal slices (Pearce, 1993). In that study, arguments were put forward indicating that a space-clamp artifact did not account for the different time courses of synaptic currents generated at different locations of the neuron. In comparison, the analysis of I_{GABA} in cultured neurons that have high input resistances (≥ 1 GΩ) and short dendrites (≤ 300 μm) recorded in the presence of TTX, QX314, and Cs^+ should be much less hindered by geometrical factors (Müller and Lux, 1993; Draguhn et al., 1997). Furthermore, the slowing of the time course of inward sIPSCs when $[K^+]_o$ was increased (Fig. 7) indicated that the time course of inward sIPSCs was shortened by superimposed small outward sIPSCs as long as the somatodendritic $[Cl^-]_i$ gradient existed.

The neuronal-specific K^+–Cl^- cotransporter is inhibited by furosemide (K_i 25 μM) (Payne, 1997). Furosemide has been used to establish the involvement of a K^+–Cl^- cotransporter in synaptic inhibition (Misgeld et al., 1986; Thompson, 1994). Furosemide, however, has various disadvantages. In non-neuronal preparations, furosemide at concentrations >0.1 mM inhibits not only cation–anion cotransporters but also other transport proteins and Cl^- channels (Cabantchik and Greger, 1992). Here we could observe immediate effects of furosemide at concentrations below 0.1 mM. Furosemide has been reported to block $GABA_A$ channels that are composed of subunits including α_4 and α_6 (Wafford et al., 1996). These subunits are uncommon in midbrain areas (Wisden et al., 1992). In neither this nor a previous study (Jarolimek et al., 1996) on midbrain culture did we obtain evidence that furosemide reduced $GABA_A$ currents. Depending on V_H, the amplitudes of IPSCs increased when neurons were exposed to furosemide, and slopes of current–voltage relationships for $GABA_A$ currents remained unaltered. As shown in the previous study (Jarolimek et al., 1996), shifts of reversal potentials of the same order of magnitude as those of E_{GABA} can be observed for glycine currents.

Furosemide blocks Na^+–K^+–Cl^- cotransporters more effectively than it blocks the K^+–Cl^- cotransporter (Cabantchik and Greger, 1992). Thus, the furosemide effects described here do not allow discrimination between the two transporters. Our data, however, exclude a significant contribution of a Na^+–K^+–Cl^-
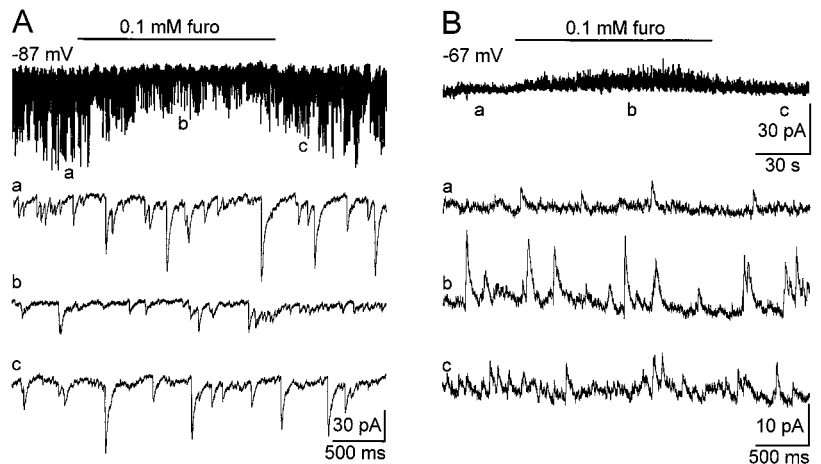
Figure 8. Under conditions of high $[K^+]_o$ and low $[A^-]_{pip}$, furosemide shifted E_{IPSC} to a more negative value. *A,* Furosemide reduced the amplitude of inward sIPSCs (recorded with 4.5 mM $[A^-]_{pip}$ and 8 mM $[K^+]_o$). *B,* In the same cell recorded under identical conditions as in *A* but at a more positive V_H, furosemide increased the amplitude of outward sIPSCs. *Letters* mark segments on the chart plots that were shown at higher sweep speed in the lower traces.
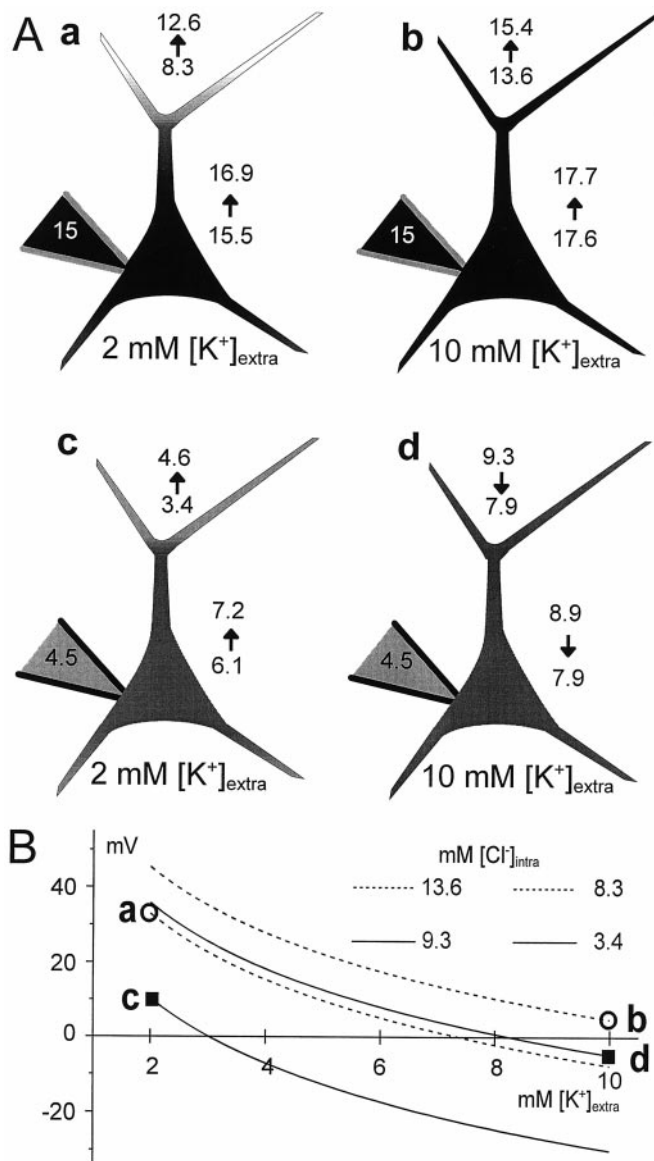
Figure 9. Cl⁻ homeostasis in cultured neurons can be explained by the operation of an electroneutral K⁺–Cl⁻ cotransporter and the Gibbs–Donnan equilibrium. *A*, $[Cl^-]_i$ was calculated from E_{GABA} listed in Table 2. Concentrations of the inorganic anions in the patch pipette were as indicated. *Arrows* indicate changes of $[A^-]_i$ calculated from changes in E_{GABA} of somatic or dendritic I_{GABA} induced by furosemide. *Letters* correspond to driving forces for the K⁺–Cl⁻ cotransporter derived from the energy profiles shown in *B*. *B*, Plot of the driving force for the K⁺–Cl⁻ cotransporter as a function of $[K^+]_o$ for different $[Cl^-]_i$ (taken from E_{GABA} calculated for dendrites in *A*). Calculations are as described in Material and Methods. Positive values indicate outward transport.

cotransporter in the net Cl⁻ transport of cultured midbrain neurons. Because of the large inwardly directed driving force for Na⁺, the driving force of the net Cl⁻ transport (Fig. 9*Ac,d*) would not reverse near $[K^+]_o$ and $[Cl^-]_i$ predicted from the driving force of a K⁺–Cl⁻ cotransporter (Fig. 9*Bc, d*).

Regulation of the neuronal Cl⁻ homeostasis by the furosemide-sensitive K⁺–Cl⁻ cotransporter

The electroneutral K⁺–Cl⁻ cotransporter operates near equilibrium under conditions of normal internal and external ion con-

centrations (Jensen et al., 1993; Payne, 1997). If $[K^+]_o$ is kept at a high level (Fig. 9*Ad*), the K⁺–Cl⁻ cotransporter accumulates Cl⁻ in the cell. Under physiological conditions, Cl⁻ accumulation would be diminished by the concomitant removal of K⁺ from the extracellular space (Payne, 1997). During epileptiform activity, however, $[K^+]_o$ has been found to remain at high levels (10–12 mM) (Heinemann and Lux, 1977), with the result that the K⁺–Cl⁻ transport actually accumulates Cl⁻ and hence intensifies epileptiform activity. Therefore, furosemide may have some antiepileptic potency under such an experimental condition (Hochman et al., 1995). In contrast, in neuronal culture we observed that furosemide induced burst activity (Jarolimek et al., 1996). In these experiments, $[K^+]_o$ was kept constant at 5 mM. In the presence of antagonists for ionotropic glutamate receptors, we observe frequent sIPSCs, suggesting that membrane potentials of the majority of cells are near to firing threshold, e.g. around −60 mV. The expected lower limit of $[Cl^-]_i$ is around 5.6 mM in 5 mM $[K^+]_o$ ($[Cl^-]_o$ = 169 mM; $[K^+]_i$ assumed to be 150 mM). There is, however, an electromotor force ($E_M - E_{Cl}$) driving Cl⁻ into the cell. The hyperpolarizing gradient for synaptic inhibition will be maintained by the outwardly directed K⁺–Cl⁻ cotransport. The upper limit of $[Cl^-]_i$ is 20 mM if the K⁺–Cl⁻ cotransporter is blocked by furosemide. Hence, in furosemide, the inhibitory potency of the GABA_A postsynaptic potentials is diminished or abolished.

CONCLUSIONS

In cultured neurons, the regulation of $[Cl^-]_i$ and the gradients for IPSCs is determined by the presence and activity of the K⁺–Cl⁻ cotransporter. The driving force for the net Cl⁻ transport is set by $[K^+]_o$ and $[Cl^-]_i$. Values determined in this study indicate that $[Cl^-]_i$ is kept well below 10 mM as long as $[K^+]_o$ is 2 mM. Increases in $[K^+]_o$ will increase $[Cl^-]_i$, but uptake of K⁺ into neurons on reversal of the transport will buffer $[K^+]_o$ changes (Payne, 1997). However, if $[K^+]_o$ remains high, the transport will accumulate Cl⁻ in the cells. *In vivo* additional factors determine gradients for IPSCs through GABA_A or glycine channels, complicating the analysis of their regulation. Despite this fact, a furosemide-sensitive K⁺–Cl⁻ cotransporter is likely to operate in central neurons because the KCC2 mRNA is expressed in hippocampal neurons (Payne et al., 1996). The permeability for HCO_3^- shifts E_{GABA} by 10–15 mV (depending on pH_i) in a positive direction (Alvarez-Leefmans, 1990; Kaila, 1994). A regulation of GABAergic inhibition through $[HCO_3^-]_i$ (Kaila, 1994) is less likely given the low permeability ratio of GABA_A receptors for HCO_3^-/Cl^- (Bormann, 1988; Fatima-Shad and Barry, 1993). Furthermore, an inwardly rectifying chloride conductance (Smith et al., 1995), which does not appear to have a major influence in our cultured neurons (Jarolimek et al., 1996), may come into play. For an excitatory effect of GABA postnatally as opposed to an inhibitory effect in adult neurons (Cherubini et al., 1991), a transient dominance of a Na⁺–K⁺–Cl⁻ cotransporter (LoTurco et al., 1995; Plotkin et al., 1997) probably coincides with a delayed expression of the K⁺–Cl⁻ cotransporter (Zhang et al., 1991).

REFERENCES

Alvarez-Leefmans FJ (1990) Intracellular Cl⁻ regulation and synaptic inhibition in vertebrate and invertebrate neurons. In: Chloride channels and carriers in neurons (Alvarez-Leefmans FJ, Russel JM, eds), pp 109–158. New York: Plenum.

Barry PH, Lynch JW (1991) Liquid junction potentials and small effects in patch-clamp analysis. J Membr Biol 121:101–117.

Bijak M, Jarolimek W, Misgeld U (1991) Effects of antagonists on quis-

qualate and nicotinic receptor-mediated currents of midbrain neurones in culture. Br J Pharmacol 102:699–705.

Bormann J (1988) Electrophysiology of GABA$_A$ and GABA$_B$ receptor subtypes. Trends Neurosci 11:112–116.

Cabantchik ZI, Greger R (1992) Chemical probes for anion transporters of mammalian cell membranes. Am J Physiol 262:C803–C827.

Cherubini E, Gaiarsa JL, Ben-Ari Y (1991) GABA: an excitatory transmitter in early postnatal life. Trends Neurosci 14:515–519.

Chesler M (1990) The regulation and modulation of pH in the nervous system. Prog Neurobiol 34:401–427.

Chesler M, Kaila K (1992) Modulation of pH by neuronal activity. Trends Neurosci 15:396–402.

Colling SB, Wheal HV (1994) Fast sodium action potentials are generated in the distal apical dendrites of rat hippocampal CA1 pyramidal cells. Neurosci Lett 172:73–76.

Connors BW, Prince DA (1982) Effects of local anesthetic QX-314 on the membrane properties of hippocampal pyramidal neurons. J Pharmacol Exp Ther 220:476–481.

Draguhn A, Pfeiffer M, Heinemann U, Polder R (1997) A simple hardware model for the direct observation of voltage-clamp performance under realistic conditions. J Neurosci Methods 78:105–113.

Fatima-Shad K, Barry PH (1993) Anion permeation in GABA- and glycine-gated channels of mammalian cultured hippocampal neurons. Proc R Soc Lond B Biol Sci 253:69–75.

Grover LM, Lambert NA, Schwartzkroin PA, Teyler TJ (1993) Role of HCO$_3^-$ ions in depolarizing GABA$_A$ receptor-mediated responses in pyramidal cells of rat hippocampus. J Neurophysiol 69:1541–1555.

Heinemann U, Lux HD (1977) Ceiling of stimulus induced rises in extracellular potassium concentration in the cerebellar cortex of the cat. Exp Brain Res 120:231–249.

Hochman DW, Baraban SC, Owens JWM, Schwartzkroin PA (1995) Dissociation of synchronization and excitability in furosemide blockade of epileptiform activity. Science 270:99–102.

Jarolimek W, Misgeld U (1991) Reduction of GABA$_A$ receptor-mediated inhibition by the non-NMDA receptor antagonist 6-cyano-7-nitroquinoxaline-2,3-dione in cultured neurons of rat brain. Neurosci Lett 121:227–230.

Jarolimek W, Misgeld U (1992) On the inhibitory actions of baclofen and γ-aminobutyric acid in rat ventral midbrain culture. J Physiol (Lond) 451:419–443.

Jarolimek W, Misgeld U (1997) GABA$_B$ receptor-mediated inhibition of tetrodotoxin-resistant GABA release in rodent hippocampal CA1 pyramidal cells. J Neurosci 17:1025–1032.

Jarolimek W, Misgeld U, Lux HD (1989) Activity dependent alkaline and acid transients in guinea pig hippocampal slices. Brain Res 505:225–232.

Jarolimek W, Brunner H, Lewen A, Misgeld U (1996) Role of chloride-homeostasis in the inhibitory control of neuronal network oscillators. J Neurophysiol 75:2654–2657.

Jensen MS, Cherubini E, Yaari Y (1993) Opponent effects of potassium on GABA$_A$-mediated postsynaptic inhibition in the rat hippocampus. J Neurophysiol 69:764–771.

Kaila K (1994) Ionic basis of GABA$_A$ receptor channel function in the nervous system. Prog Neurobiol 42:489–537.

Kaila K, Lamsa K, Smirnov S, Taira T, Voipio J (1997) Long-lasting GABA-mediated depolarization evoked by high-frequency stimulation in pyramidal neurons of rat hippocampal slice is attributable to a network-driven, bicarbonate-dependent K⁺ transient. J Neurosci 17:7662–7672.

LoTurco JL, Owens DF, Heath MJS, Davies MBE, Kriegstein AR (1995) GABA and glutamate depolarize cortical progenitor cells and inhibit DNA synthesis. Neuron 15:1287–1298.

Misgeld U, Deisz RA, Dodt HU, Lux HD (1986) The role of chloride transport in postsynaptic inhibition of hippocampal neurons. Science 232:1413–1415.

Müller W, Lux HD (1993) Analysis of voltage-dependent membrane currents in spatially extended neurons from point clamp data. J Neurophysiol 69:241–247.

Nathan T, Jensen MS, Lambert JDC (1990) The slow inhibitory postsynaptic potential in rat hippocampal CA1 neurones is blocked by intracellular injection of QX-314. Neurosci Lett 110:309–313.

Neher E (1992) Correction for liquid junction potentials in patch clamp experiments. In: Methods in enzymology, Vol 207, pp. 123–131. New York: Academic.

Payne JA (1997) Functional characterization of the neuronal-specific K-Cl cotransporter: implications for [K⁺]$_o$ regulation. Am J Physiol 273:C1516–C1525.

Payne JA, Stevenson TJ, Donaldson LF (1996) Molecular characterization of a putative K-Cl cotransporter in rat brain. J Biol Chem 271:16245–16252.

Pearce RA (1993) Physiological evidence for two distinct GABA$_A$ responses in rat hippocampus. Neuron 10:189–200.

Perkins PL, Wong RK (1996) Ionic basis of the depolarizing GABA response in hippocampal pyramidal cells. J Neurophysiol 76:3886–3894.

Plotkin MD, Snyder EY, Hebert SC, Delpire E (1997) Expression of the Na-K-2Cl cotransporter is developmentally regulated in postnatal rat brains: a possible mechanism underlying GABA's excitatory role in immature brain. J Neurobiol 33:781–795.

Raley-Susman KM, Sapolsky RM, Kopito RR (1993) Cl⁻/HCO$_3^-$ exchange function differs in adult and fetal rat hippocampal neurons. Brain Res 614:308–314.

Rohrbacher J, Krieglstein K, Honerkamp S, Lewen A, Misgeld U (1995) 5,7-Dihydroxytryptamine uptake discriminates living serotonergic cells from dopaminergic cells in rat midbrain culture. Neurosci Lett 199:207–210.

Rohrbacher J, Jarolimek W, Lewen A, Misgeld U (1997) GABA$_B$ receptor-mediated inhibition of spontaneous inhibitory synaptic currents in rat midbrain culture. J Physiol (Lond) 500:739–749.

Sivilotti L, Nistri A (1991) GABA receptor mechanisms in the central nervous system. Prog Neurobiol 36:35–92.

Smith RL, Clayton GH, Wilcox CL, Escuerdo KW, Staley KJ (1995) Differential expression of an inwardly rectifying chloride conductance in rat brain neurons: a potential mechanism for cell-specific modulation of post-synaptic inhibition. J Neurosci 15:4057–4067.

Staley KJ, Soldo BL, Proctor WR (1995) Ionic mechanisms of neuronal excitation by inhibitory GABA$_A$ receptors. Science 269:977–981.

Thompson SM (1994) Modulation of inhibitory synaptic transmission in the hippocampus. Prog Neurobiol 42:575–609.

Wafford KA, Thompson SA, Sikela J, Wilcox AS, Whiting PJ (1996) Functional characterization of human gamma-aminobutyric acid(a) receptors containing the alpha-4 subunit. Mol Pharmacol 50:670–678.

Wisden W, Laurie DJ, Monyer H, Seeburg PH (1992) The distribution of 13 GABA$_A$ receptor subunit messenger RNAs in the rat brain. 1. Telencephalon: diencephalon, mesencephalon. J Neurosci 12:1040–1062.

Zhang L, Spigelman I, Carlen PL (1991) Development of GABA-mediated, chloride-dependent inhibition in CA1 pyramidal neurones of immature rat hippocampal slices. J Physiol (Lond) 444:25–49.